CORE
Metadata, citation and similar papers at core.ac.uk
Provided by Elsevier - Publisher Connector

Virology 413 (2011) 118–127

Contents lists available at ScienceDirect

Virology

journal homepage: www.elsevier.com/locate/yviro

Amino acid changes within the E protein hinge region that affect dengue virus type 2 infectivity and fusion

Siritorn Butrapet [a,1], Thomas Childers [a], Kelley J. Moss [a,2], Steven M. Erb [b], Betty E. Luy [a], Amanda E. Calvert [a], Carol D. Blair [b], John T. Roehrig [a], Claire Y.-H. Huang [a,*]

[a] Division of Vector-Borne Diseases, Centers for Disease Control and Prevention, Fort Collins, CO 80521, USA
[b] Arthropod-borne and Infectious Diseases Laboratory, Department of Microbiology, Immunology, and Pathology, Colorado State University, Fort Collins, CO 80523, USA

ARTICLE INFO

Article history:
Received 11 November 2010
Returned to author for revision
12 December 2010
Accepted 24 January 2011
Available online 24 February 2011

Keywords:
Dengue virus
Flavivirus
Hinge
Fusion
Envelope protein
Mutagenesis

ABSTRACT

Fifteen mutant dengue viruses were engineered and used to identify AAs in the molecular hinge of the envelope protein that are critical to viral infection. Substitutions at Q52, A54, or E133 reduced infectivity in mammalian cells and altered the pH threshold of fusion. Mutations at F193, G266, I270, or G281 affected viral replication in mammalian and mosquito cells, but only I270W had reduced fusion activity. T280Y affected the pH threshold for fusion and reduced replication in C6/36 cells. Three different mutations at L135 were lethal in mammalian cells. Among them, L135G abrogated fusion and reduced replication in C6/36 cells, but only slightly reduced the mosquito infection rate. Conversely, L135W replicated well in C6/36 cells, but had the lowest mosquito infection rate. Possible interactions between hinge residues 52 and 277, or among 53, 135, 170, 186, 265, and 276 required for hinge function were discovered by sequence analysis to identify compensatory mutations.

Published by Elsevier Inc.

Introduction

Dengue is the most important mosquito-borne viral disease in the world, with over 2.5 billion people living in more than 100 endemic countries at risk. Up to 100 million infections occur annually with 500,000 cases of severe dengue hemorrhagic fever/dengue shock syndrome, and 22,000 deaths, mainly among children (http://www.who.int/csr/disease/dengue/impact). Dengue viruses (DENVs) are transmitted by *Aedes* spp. mosquitoes, principally *Ae. aegypti*, and there are 4 distinct serotypes (types 1–4; DENV1–4) within the DENV serocomplex of genus *Flavivirus*, family *Flaviviridae*. The mature flavivirus is approximately 500 Å in diameter and has a capsid (C) protein core complexed with a single-stranded positive-sense RNA genome (~11 kb). The core is surrounded by a lipid bilayer in which 180 copies each of the viral envelope (E) protein and membrane (M) protein are embedded. The E proteins are arranged in an icosahedral scaffold of 90 homodimers that are complexed with the M protein (Kuhn et al., 2002). The E protein is a class II fusion protein, essential for host cell attachment, entry, viral-endosome membrane fusion, and virus assembly.

Following attachment, the virion is internalized mainly via receptor-mediated, clathrin-dependent endocytosis (Chu and Ng, 2004; Gollins and Porterfield, 1985; Mosso et al., 2008; van der Schaar et al., 2008). The lower pH in the endosomes triggers an oligomeric rearrangement of the E protein from homodimers to homotrimers (Bressanelli et al., 2004; Modis et al., 2004; Stiasny et al., 2004). During the rearrangement, pre-fusion E dimers dissociate to intermediate monomers with exposed fusion peptides (FPs) that can interact with endosome membranes. Subsequently, the E monomers form post-fusion homotrimers, bringing into contact the C-terminal membrane anchor of the E protein with the FP-inserted endosome membrane (Stiasny et al., 2007). After membrane fusion, viral nucleocapsid escapes from the endosome and initiates viral replication.

Solved structures of the soluble flavivirus E protein ectodomain crystals revealed three domains (DI, DII, and DIII) (Modis et al., 2003, 2005; Rey et al., 1995), which correlate to the previously defined antigenic domains C, A, and B (Heinz, 1986; Mandl et al., 1989; Roehrig et al., 1990). DIII is connected to DI by a single peptide strand. DI and DII are linearly discontinuous structures connected by four peptide strands that function as a "molecular hinge (H)" during low pH-induced E protein reorganization to facilitate viral fusion with endosomal membranes (Rey et al., 1995). The four loosely packed DI-DII interface peptides, designated H-1 to H4 (Hurrelbrink and McMinn, 2001), provide flexibility for the low-pH catalyzed E conformational changes. Further evidence of the hinge role included mutations at this region affecting viral virulence and/or the pH threshold for fusion (Cecilia and

* Corresponding author at: Arbovirus Diseases Branch, Division of Vector-Borne Diseases, Centers for Disease Control and Prevention, 3150 Rampart Road, Ft Collins, CO 80521, USA.
E-mail addresses: yxh0@cdc.gov, CHuang1@cdc.gov (C.Y.-H. Huang).
[1] Current Address: University of Liverpool, Delby Street, Liverpool L69 3GA, UK.
[2] Current Address: University of Wyoming, 1000 East University Avenue, Laramie, WY 81, USA.

0042-6822/$ – see front matter. Published by Elsevier Inc.
doi:10.1016/j.virol.2011.01.030

Gould, 1991; Hurrelbrink and McMinn, 2001; Lee et al., 1997; Monath et al., 2002), as well as the change in orientation between the DENV pre-fusion and post-fusion crystal structures (Modis et al., 2003, 2004). Comparison between the crystal structures of the E monomers of mature and immature virions demonstrated a rotation around the hinge region, suggesting the hinge motions are also essential for the virus maturation process (Zhang et al., 2004). In addition, a stem consisting of two α-helices that links the soluble ectodomain and trans-membrane domain of the E protein is likely to contribute further flexibility required for the conformational change (Zhang et al., 2003).

Recently, we reported detailed mutagenesis studies of the DENV2 E protein DII FP (Huang et al., 2010) and DIII FG loop (Erb et al., 2010). In this report, we identified AAs within the hinge region of DENV2 that are critical for viral replication and fusion. We engineered 15 DENV2 mutants by introducing distinct mutations at two residues each in H-1 to H-3 and at 5 residues in H4 into cDNA infectious clones. Through analysis of the mutation effects on growth in cell cultures and *Aedes aegypti* mosquitoes, membrane fusion efficiency and pH threshold, thermal stability, and reactivity with E protein specific monoclonal antibodies (MAbs), we identified nine residues within the E protein H peptides that are important for DENV2 replication.

Results

Design and construction of mutant viruses

Our mutagenesis targets were designed to determine the importance of highly conserved AA residues, the side-chain size of these residues, and the biochemical properties of the residues in maintaining the function of the E protein molecular hinge. Identification of AAs within the DENV2 H region (Fig. 1), H-1: AA 51–54 (E residues), H-2: AA 130–135, H-3: AA 186–196, and H4: AA 265–283, was based on the DENV2 E protein crystal structure (Modis et al., 2003). The 4 hinge peptides exhibit different levels of homology among flaviviruses

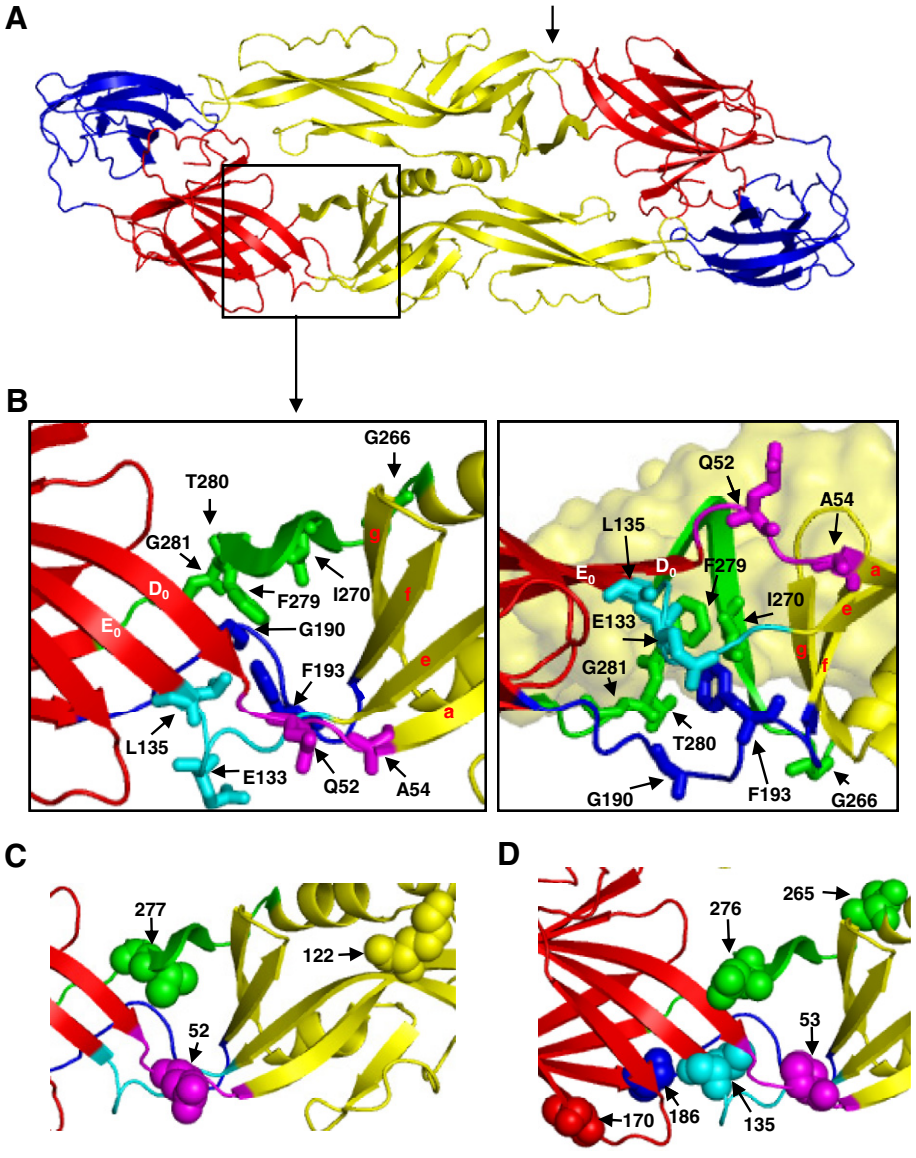

Fig. 1. Atomic structure of DENV2 envelope protein hinge region. (A) Top-view of E protein homodimer structure on mature virion. The glycosyl chains of the E protein are not shown. Arrow indicates hinge region on one monomer. (B) Eleven amino acid residues of the hinge region targeted for mutagenesis in this study are marked. Left panel: Top-view of hinge region. Right: Side-view of hinge region. The β-sheets DI-D_0E_0 and DII-gfea are marked with white or red letters. (C) Positions of compensatory mutations evolved during growth of mutant Q52R mutant. (D) Positions of compensatory mutations evolved during growth of mutants L135W and L135K. Structures of the E protein homodimer (ID: 1oan) were obtained from protein database bank and rendered by Polyview-3D to add annotations. E protein domains are shown as DI-red, DII-yellow, and DIII-blue. Hinge peptides are shown as H-1 in magenta, H-2 in cyan blue, H-3 in dark blue, and H-4 in green.

Table 1
Amino acid sequence alignment of E protein hinge region peptides among flaviviruses.

Virus[a]	H-1(E51-54)[b]				H-2 (E130-135)[b]						H-3(E186-196)[b]										
DENV2 16681	K	**Q**	P	**A**	V	Q	P	**E**	N	**L**	S	P	R	T	**G**	L	D	**F**	N	E	M
DENV1 16007	T	N	•	•	•	•	Y	•	•	•	•	•	•	•	•	•	•	•	•	•	•
DENV3 16562	T	•	L	•	•	•	H	•	•	•	•	•	•	•	•	•	•	•	•	•	•
DENV4 1036	•	E	V	•	•	•	I	•	•	•	E	•	•	S	•	I	•	•	•	•	•
JEV JaOArS982	S	•	L	•	I	•	•	•	•	I	E	•	•	S	•	•	N	T	E	A	F
WNV NY99	A	N	L	•	I	L	K	•	•	I	E	•	•	S	•	I	•	T	•	A	Y
MVEV	T	N	L	•	I	L	•	•	D	I	E	•	•	S	•	•	N	T	E	A	Y
SLEV MSI7	T	E	L	•	I	L	R	•	•	I	E	A	•	S	•	I	N	T	E	D	Y
YFV Asibi	D	G	•	•	•	D	Q	T	K	I	Q	V	Q	•	A	V	•	•	G	N	S
TBEV Neudoerfl	E	N	•	•	Y	D	A	N	K	I	R	V	A	S	•	V	•	L	A	Q	T
LGTV TP21	E	S	•	•	Y	D	V	N	K	I	R	V	A	S	•	V	•	L	A	Q	T
POWV LB	E	S	•	•	Y	D	S	T	K	I	R	V	A	S	•	I	•	V	A	Q	T

Virus	H-4 (E265-283)[b]																						
DENV2 16681	T	**G**	A	T	E	**I**	Q	M	S	S	G	N	L	–	–	–	L	**F**	**T**	–	**G**	H	L
DENV1 16007	•	•	•	•	•	•	•	T	•	G	T	T	T	–	–	–	I	•	A	–	•	•	•
DENV3 16562	•	•	•	•	•	•	•	T	•	G	G	T	S	–	–	–	I	•	A	–	•	•	•
DENV4 1036	A	•	•	•	•	V	D	S	G	D	G	•	H	–	–	–	M	•	A	–	•	•	•
JEV JaOArS982	A	•	•	I	V	V	E	Y	•	•	S	–	V	–	–	–	K	L	•	S	•	•	•
WNV NY99	A	•	•	I	P	V	E	F	•	•	N	T	V	–	–	–	K	L	•	S	•	•	•
MVEV	A	•	•	I	P	V	E	F	•	•	S	T	•	–	–	–	K	L	•	S	•	•	•
SLEV MSI7	A	•	•	I	P	A	T	V	•	•	S	T	•	–	–	–	T	L	Q	S	•	•	•
YFV Asibi	T	•	•	M	R	V	T	K	D	T	N	D	N	N	L	Y	K	L	H	G	•	•	V
TBEV Neudoerfl	A	•	–	–	–	V	P	V	A	H	I	E	G	T	K	Y	H	L	K	S	•	•	V
LGTV TP21	A	•	–	–	–	V	P	V	A	•	I	E	G	T	K	Y	H	L	K	S	•	•	V
POWV LB	A	•	–	–	–	V	P	L	A	•	V	E	G	Q	K	Y	H	L	K	S	•	•	V

[a] Assesion numbers: U87411 (DENV2), AF180818 (DENV1), M18370 (JEV), AF196835 (WNV: West Nile virus), X03467 (MVEV: Murray Valley encephalitis virus), AY289618 (SLEV: St. Louis encephalitis virus), AY640589 (YFV), U27495 (TBEV: tick-borne encephalitis virus), AF253419 (LGTV: Langat virus), L06436 (POWV: Powassan virus).
[b] AA positions of DENV2 E protein. Bold letters: Target DENV2 AA for mutations. Alignment: •, AA is the same as DENV2; –, no AA.

(Table 1). H-1 consists of two hydrophilic residues at 51–52 and hydrophobic residues at 53–54. We made a mutation at Q52 to R, which has been speculated to be involved in mouse attenuation in conjunction with other mutations in yellow fever virus (YFV) 17D vaccine (Schlesinger et al., 1996) and a Japanese encephalitis virus (JEV) mutant (Hasegawa et al., 1992). The A54, located near the N-terminus of a DII β-sheet, is highly conserved among flaviviruses (Table 1), and we substituted the small hydrophobic residue with a large acidic residue (A54E) to investigate the importance of this conservation. Mutation of the wild-type (wt) YFV French viscerotropic virus (FVV) A54 to V in the French neurotropic vaccine (FNV) was postulated to be one of the E protein mutations contributing to the attenuation phenotype of FNV (Ni et al., 2000; Wang et al., 1995). In H-2, E133 is conserved among the mosquito-borne flaviviruses and residue 135 (L or I) is highly conserved among all flaviviruses. We made a charge change from an acidic E to a basic K for residue 133 and for L135, mutations to W (larger hydrophobic), G (no side chain), or K (basic) were generated to investigate the effect of size and hydrophobicity on this AA. In H-3, we changed the highly conserved G190 to much larger side-chain F or W. We also targeted the large hydrophobic F193 that is conserved among all four serotypes of DENV and changed it to a smaller hydrophobic A or a basic R. DENV3 containing a mutation at this residue showed a marked decrease in fusion pH threshold (Lee et al., 1997). H4 contains highly variable AA primary sequences among the flaviviruses, and is the longest linker of the hinge region. We substituted the conserved G266, I270, or G281 to the larger W in each case. The F279 is conserved among the DENVs and a F277S mutation in DENV3 (equivalent to F279 in DENV2) has been shown to decrease the fusion pH threshold. We changed F279 to a smaller A in our study. A semi-conserved small residue, T280, was also targeted for a substitution with a much larger Y.

Viability of the mutant viruses

All 15 hinge mutations resulted in viable mutant viruses recovered from transfected Vero and/or C6/36 cells, with working seed titers ranging from 5.03 to 7.95 $\log_{10}$ $TCID_{50}$/ml (measured in C6/36 cells). Full-genome sequences of all recovered working seeds were determined, and only the viruses with accurate genome sequences were used for subsequent phenotypic characterizations. In Vero cells, eight mutants, including two lethal (no virus recovered after multiple transfection efforts) and six unstable mutants (virus recovered with reversion and/or extra non-synonymous mutation), were considered nonviable (Table 2). Interestingly, virus recovered from the L135K mutation acquired a substitution that changed the engineered K to M. Mutants E133K, L135W, and G266W showed reversion at the mutation site in the recovered virus seeds. Mutant I270W retained the correct mutation, but acquired additional mutations at K64M and K122I. The extra K122I mutation was also found in revertants of mutants E133K and G266W. In fact, the additional K122I or K122E mutations were identified in other mutants we reported previously (Erb et al., 2010) as well as in several wt DENV2 16681 seeds passaged in Vero cells (unpublished data). In contrast, all the eight nonviable mutants in Vero cells produced infectious viruses from C6/36 cells with expected full-length genome sequences.

Growth kinetics of the mutant viruses

Growth kinetics of the mutant viruses were analyzed in Vero, HepG2, K562, and C6/36 cells for 12–14 days by measuring viral RNA in culture medium by qRT-PCR. Since some mutant viruses did not replicate or produce plaques in Vero cells, infectious virus titer in growth medium at the peak day of viral RNA release for each mutant was measured by 50% tissue culture infectious dose ($TCID_{50}$) assay in C6/36 cells. All mutant viruses replicated similarly to wt 30P-NBX virus (clone-derived DENV2 16681) in C6/36 cells, with exponential RNA increase between day 0 and day 6, and reached plateau titers around 10–11 $\log_{10}$ copies/ml between day 6 and day 14 (data not shown). However, the infectious virus titers measured at the peak viral RNA time points were lower than parental virus for seven mutant viruses, L135G, L135K, F193R, G266W, I270W, T280Y, and G281W (Fig 2A).

In Vero cells, growth kinetics of mutants G190F, G190W, F279A and T280Y were similar to control 30P-NBX virus (Fig. 2B). Mutants

Table 2
Viability, genome sequence, and fusion capacity of the clone-derived hinge region mutant viruses.

Virus	Vero cells		C6/36 cells		Fusion	
	Viability[a]	Sequence[b]	Viability[a]	Sequence[b]	Activity at pH 5.5[c]	pH Threshold
30P-NBX	+	Correct	+	Correct	1 ± 0.15	6.3–6.5
Q52R	+	Correct	nd	na	1.06 ± 0.29	6.5–6.8
A54E	+	Correct	nd	na	1.02 ± 0.24	≥6.8
E133K	−	Rev + K122I	+	Correct	1.14 ± 0.03	≥6.8
L135W	−	Rev	+	Correct	1.23 ± 0.22*	≥6.8
L135G	−	No virus	+	Correct	0.05 ± 0.07**	−
L135K	−	L135M	+	Correct	0.95 ± 0.05	6.3–6.5
G190F	+	Correct	nd	na	1.10 ± 0.03	6.3–6.5
G190W	+	Correct	nd	na	1.01 ± 0.10	≥6.8
F193A	+	Correct	nd	na	1.27 ± 0.23*	6.5–6.8
F193R	−	F193L/R	+	Correct	1.06 ± 0.02	6.3–6.5
G266W	−	Rev + K122I	+	Correct	0.90 ± 0.20	6.3–6.5
I270W	±	+ K64M + K122I	+	Correct	1.02 ± 0.08	6.0–6.3
F279A	+	Correct	+	Correct	0.86 ± 0.22	6.3–6.5
T280Y	+	Correct	nd	na	0.77 ± 0.11*	6.0–6.3
G281W	−	No virus	+	Correct	1.10 ± 0.19	6.3–6.5

[a] Viability: + virus recovered from transfected cells. − Either no virus recovered or recovered virus had reversion or mutations at the target site. ± recovered virus had correct mutation at target site, but acquired additional E mutations. nd: not done.
[b] Full-length genome sequence of clone-derived viruses: correct genome sequence (correct), reverted to wt (Rev), recovered with different substitution at the mutation site (shown), or contained the engineered mutation plus substitution(s) at different E protein residue(s) (shown as +). There were no mutations in other genes. na: not applicable.
[c] Fusion activity (± standard deviation) normalized to clone-derived wt D2-30P-NBX virus at pH 5.5 (calibrated fusion index of wt control in each experiment = 1); standard deviation for wt was calculated from all wt controls included in experiments. Student's *t*-test *$p<0.05$, **$p<0.0005$.

A54E and F193A showed somewhat lower replication efficiency than the control virus. Mutant Q52R also replicated similarly to the wt virus up to day 8, but the titers dropped on day 10. Both growth curve cultures of Q52R showed significantly more cytopathic effects (CPE) than the wt and other mutant viruses on day 8–12, suggesting the decreased virus titers after day 10 may be the result of significant cell death. Most of these viruses were viable and seemed to be genetically stable in Vero cells after 2 passages (Table 2), but we found that at day 12 of the growth curve, virus released by mutant Q52R had acquired two additional partial mutations (mixed consensus sequences detected), K122I/K and L277L/S. Notably, AA 277 is close to AA 52 in the E protein crystal structure (Fig. 1C). This suggests that the Q52R mutation affected replication in Vero cells, even though it was not easily detected by growth kinetics at early stages, leading to accumulation of compensatory and cell-adaptive mutations that enhanced viral replication. It is likely the replication enhancement also led to greater CPE in the cells, resulting in significantly decreased viral genomic titers at later time points.

Interestingly, mutant L135G failed to replicate in Vero cells, and the remaining seven mutant viruses showed significant delays in viral replication for 4–6 days (Fig. 2C). The seven mutants with delayed replication eventually broke through after day 6, and genome sequence analysis of the day 12 samples from these growth curves revealed that two mutants, G266W, and G281W, had almost fully reverted to the wt sequence. The mutant E133K sample harvested on day12 revealed mixed sequences at the engineered mutation site, with either wt reversion or 133Q substitution. The day 12 sample of mutant L135W had not reverted to wt as previously found in Vero cell-derived virus (Table 2), but had acquired two additional mutations in or near the hinge region, P53L/P (mixed sequence population) and T170A (Fig. 1D). The day 12 sample of mutant I270W had the same additional mutations (K64M/K and K122I/K) that were found in the Vero cell-derived I270W mutant virus seed (Table 2). Similarly, the L135K and F193R mutants evolved to L135M and F193L, respectively, during the growth curve study, which is consistent with the changes observed in deriving these mutants from Vero cells (Table 2). In addition to the evolved L135M mutation, the day 12 sample of L135K revealed mutation T265T/S, located at the end of H-4 (Fig. 1D).

To further investigate the growth kinetics of the mutants in different mammalian cell types, we conducted growth curve studies in HepG2 and K562 cells. Both HepG2 cells (hepatocytes) and K562 cells (leukemia cells) were human cells that are highly susceptible to DENV infection and have been widely used in study of DENV infection. Growth curves in HepG2 and K562 showed similar results as in Vero cells (data not shown). The control 30P-NBX virus replicated to peak titers of 6–7 $\log_{10}$ $TCID_{50}$/ml in these cells. Mutation L135G was lethal in all mammalian cells tested. Mutants that showed suboptimal or delayed replication in Vero cells also grew poorly in HepG2 and K562 cells. In fact, many of the mutant viruses did not replicate to sufficient titers in HepG2 cells for genome sequencing. Partial or full reversion and/or unexpected substitutions identified in the Vero cell day 12 growth curve samples of mutants E133K, L135K, F193A, G266W, and G281W were also found in the day 12 samples of the K562 cell growth kinetics study. Although the day 12 Vero cell growth curve sample of mutant Q52R showed extra mutations, the mutant maintained correct genome sequence in K562 and HepG2 cells. Interestingly, mutant L135W grown in K562 cells evolved additional mutations S186F/S and N276N/Y, which were different from those identified in the Vero cell day 12 sample. However, these two mutations also mapped to the hinge region (Fig. 1D), suggesting they may be compensatory mutations.

Temperature sensitivity of the hinge mutants

To determine whether the different incubation temperatures for mammalian cells (37 °C) and C6/36 cells (28 °C) contributed to the radical difference in the viability and genetic stability of eight mutant viruses, E133K, L135G, L135W, L135K, F193R, G266W, I270W, and G281W, we examined growth kinetics of these mutants in Vero cells at 28 °C (data not shown). Except for mutant L135G, all mutants and the wt 30P-NBX viruses replicated slower and reached lower peak titers at 28 °C compared to their growth at 37 °C. Genomic sequences of the 28 °C day 12 samples of Q52R, E133K, and I270W revealed similar extra mutations or wt reversion to those observed in the 37 °C growth curve study, indicating that the lower temperature did not abrogate the instability of these mutants in Vero cells. Although extra substitutions or reversion were not found at day 12 in the 28 °C samples of mutants L135W, L135K, F193R, G266W, and G281W, we cannot rule out the possibility that cell-adaptation mutations or reversions were present but not yet detectable because of their very low titers.

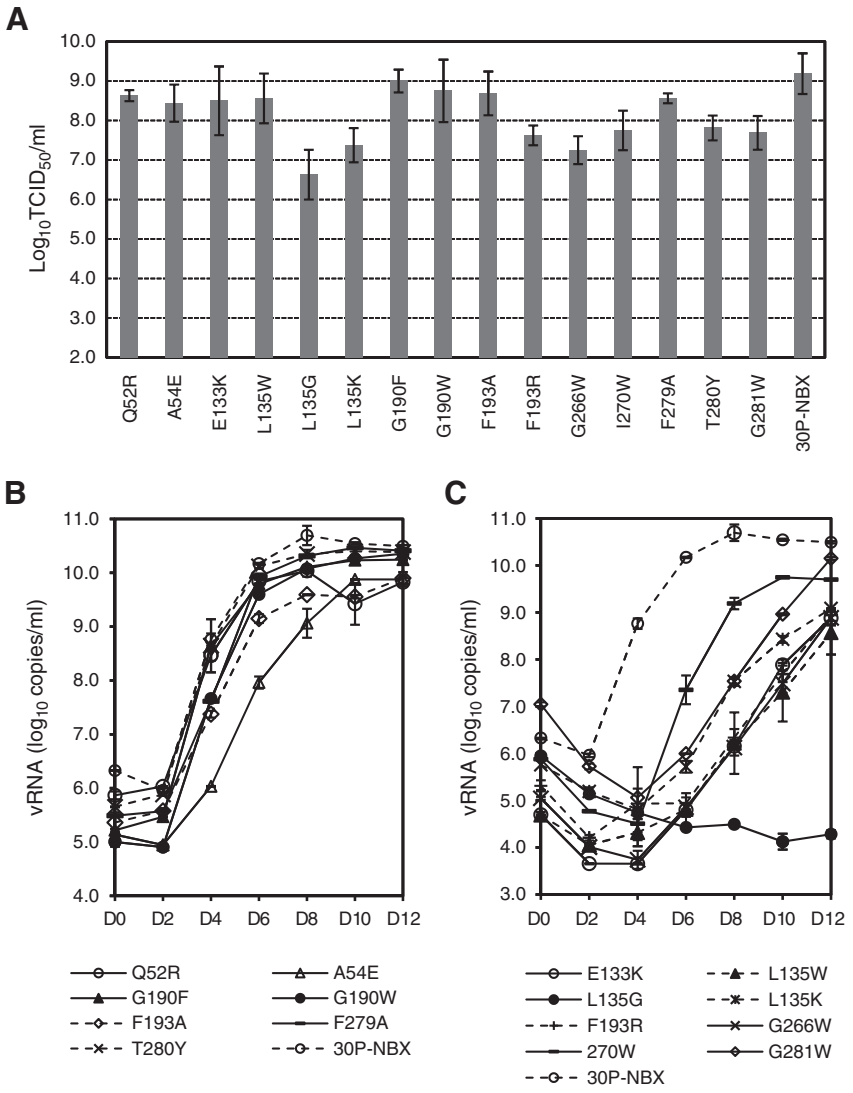

Fig. 2. Virus replication in C6/36 cells or Vero cells. (A) Peak titers of mutant and wt viruses during replication in C6/36 cell cultures. (B and C) Growth kinetics of the viruses in Vero cells. Virus growth was monitored by qRT-PCR of viral RNA in culture medium every two days. Time points with peak viral RNA were assayed for infectivity by $TCID_{50}$. Error bars represent duplicate experimental results.

Interestingly, the L135G virus that was nonviable at 37 °C was able to replicate in Vero cells at 28 °C. It reached titers about 10-fold lower than the wt virus, and no evidence of extra E-gene mutations was found after 12 days' growth at 28 °C. It appeared that the L135G substitution significantly decreased viral thermal stability at 37 °C. To further investigate the profound effect of the L135G mutation on viral thermal stability, we conducted temperature shift experiments in Vero cells to analyze the temperature effect at different stages of the virus replication. As expected, shift of the wt virus-infected culture to 37 °C after 28 °C adsorption significantly enhanced virus replication (Fig. 3A), while temperature shift to 28 °C after 37 °C adsorption caused slower virus replication (Fig. 3C). In contrast, temperature shift to 37 °C after adsorption at 28 °C significantly abrogated mutant L135G replication (Fig. 3A), while shift of the temperature to 28 °C after adsorption at 37 °C resulted in restoration of L135G virus replication in Vero cells (Fig. 3C). Measurement of intracellular negative-strand viral RNA of mutant L135G showed an increase within 48 h after infection in all temperature combinations (Fig. 3B and D). However, after 48 h the amount of negative-strand RNA in the L135G-infected cells that were maintained at or shifted to 37 °C dropped to a lower level than those cultures maintained at or shifted to 28 °C (Fig. 3B and D). These results indicated that mutant L135G was competent in cell attachment/entry and initiation of viral RNA replication in Vero cells at either temperature, but its thermal instability at 37 °C affected later stages of virus replication. Since the titers of L135G were 10-fold less than wt virus, even when grown at 28 °C, decreased thermal stability may only be part of the cause of its replication deficiency in Vero cells.

Replication of the mutants in Aedes aegypti mosquitoes

Although all the mutant viruses replicated reasonably well in mosquito C6/36 cells, it is important to assess their infectivity in intact *Ae. aegypti* mosquitoes to understand the importance of E protein hinge function in infection of and transmission by the vector. We chose the three mutants targeted at L135 for mosquito inoculation, because this set includes mutant L135W, with replication comparable to wt 30P-NBX, and two mutants, L135G and L135K, that replicated to significantly lower titers in our C6/36 cell growth curve study (Fig. 2A). We also included mutant L135M, which was recovered from Vero cells when we were attempting to derive L135K (evolved from 135K to 135M), to determine whether the Vero cell-adaptation substitution would increase the virus fitness in mosquitoes. Interestingly, the most C6/36 cell-compatible L135W virus had the lowest

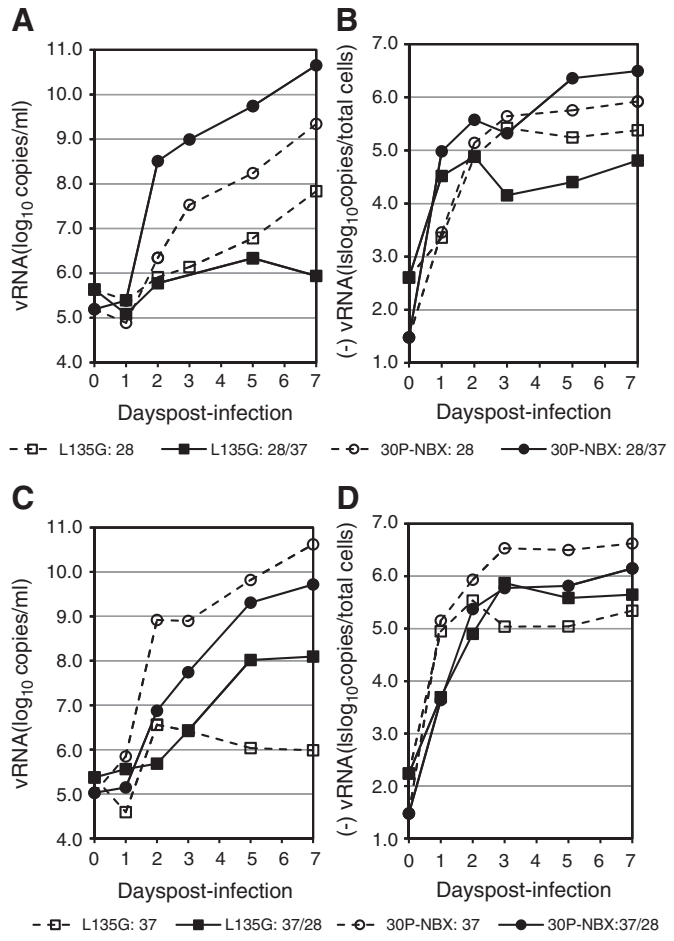

Fig. 3. Temperature shift experiments with L135G and wt viruses. Top panels (A) and (B): After viral adsorption at 28 °C for 2 h, a set of cultures were maintained at 28 °C (L135G: 28 and 30P-NBX: 28) while a duplicate set was moved to 37 °C (L135G: 28/37 and 30P-NBX: 28/37) for 7 days. Bottom panels (C) and (D): Virus adsorption at 37 °C for 2 h, a set of cultures was then maintained at 37 °C (L135G:37 and 30P-NBX: 37) while a duplicate set was moved to 28 °C (L135G: 37/28 and 30P-NBX: 37/28). (A) and (C) show measurement of viral RNA in cell culture medium. (B) and (D) show measurement of intracellular negative-strand viral RNA.

infection rate in *Ae. aegypti* mosquitoes (Table 3) via intrathoracic inoculation. The infection rate of mutant L135K was also significantly ($p = 0.017$) less than the wt virus, while the Vero cell-adapted mutant L135M had a similar infection rate to the wt virus in mosquitoes. There also was a difference between the mosquito infection rates of wt virus and mutant L135G ($p = 0.05$), which did not replicate in Vero cells and replicated most poorly of all mutants in C6/36 cells. However, because the fusion-incompetent L135G was still able to infect 74.75% of mosquitoes, we examined its E-gene sequence after replication in mosquitoes and confirmed that the L135G mutation was retained without other compensatory E mutations.

Table 3
Infectivity of the L135 mutant viruses for *Ae. aegypti* RexD mosquitoes.

	Infection rate (%)		Total numbers		
Virus	Average	SD	Mosquitoes	Experiments	p^*
30P-NBX	95.01	4.12	143	5	
L135W	11.83	9.57	162	5	<0.0001
L135G	74.75	12.87	98	3	0.052
L135K	81.65	5.73	89	3	0.017
L135M	92.59	12.83	94	3	0.389

* Probability value in Student's *t*-test (two-tailed, unpaired, unequal variance) comparing the mutants to wt 30P-NBX.

Fusion efficiency of the mutants

Fusion-from-within (FFWI) assays in C6/36 cells were conducted over a range between pH6.0 and pH6.8 to assess the effect of the hinge mutations in virus-mediated cell membrane fusion. All mutants replicated reasonably well in C6/36 cells after infection at MOI of 0.001 (Fig. 2A), indicating that this cell line is suitable for the FFWI assay. To further ensure that the assay was conducted when sufficient E proteins were expressed by each mutant, cells were infected with a higher MOI (0.1; 100×-fold higher than for growth curves) and incubated for 7 days before the FFWI assay. Table 2 lists the fusion activity normalized to wt fusion at pH5.5 and the pH threshold range for each mutant. Fig. 4 shows examples of the five patterns of fusion curves we observed, including a previously reported fusion-defective mutant, G104S, containing a mutation in the fusion loop (Huang et al., 2010) as a negative control. Pattern 1, fusion pH threshold at pH 6.3–6.5 (similar curve as wt virus), includes L135K, G190F, F193R, G266W, F279A, and G281W. Pattern 2, slightly lower fusion pH threshold (pH 6.0–6.3) than wt virus, includes I270W and T280Y. Pattern 3, slightly higher fusion pH threshold (pH 6.5–6.8) than wt virus, includes Q52 and F193A. Pattern 4, fusion pH threshold ≥ pH 6.8, includes A54E, E133K, L135W, and G190W. Pattern 5, fusion defective at all pH, is characteristic of only mutant L135G.

Antibody epitopes of the mutant viruses

A panel of well characterized murine MAbs was used to analyze the E protein epitopes of hinge mutants expressed in C6/36 cells at 28 °C. Most mutants showed similar reactivity to all the tested MAbs as the wt E protein (data not shown). Substitution of the L135 residue with K or G reduced the E protein reactivity with the DI MAb 1B4C-2, by 3-fold (L135K) or 4-fold (L135G). Changing L135 to either W or M had no effect on 1B4C-2 reactivity. H-4 mutations at either G266 or F279 reduced the reactivity of the DII MAb 2H3 (A4 epitope) by 3-fold. The F193R mutation reduced the reactivity of the DIII MAb 9A3D-8 (B2 epitope) by 3-fold.

To further investigate the effect of the temperature sensitivity mutation L135G on the expression of E protein epitopes, we compared the MAb reactivity with the mutant E protein expressed in Vero cells at 28 and 37 °C. Significantly reduced reactivity to MAbs that recognize A1, A4, A5, B2, or C1 epitopes, located in all three E domains (Table 4), was observed for mutant L135G-infected cells at 37 °C when compared to the reactivity of 28 °C infected cells. On the other hand, the wt viral E protein expressed in 28 °C and 37 °C did not show significant difference in its reactivity with any of the tested MAbs (data not shown).

Discussion

The H region of the flavivirus E protein consists of 4 loosely packed peptide linkers between the DI-D_0E_0 and DII-gfea β-sheets (Fig. 1B). This region and its nearby loop structures are highly susceptible to adaptive mutations during passage in cultured cells and mouse brains (Bray et al., 1998; Duarte dos Santos et al., 2000; Hasegawa et al., 1992; Lee et al., 1997; McMinn et al., 1995b; Monath et al., 2002; Schlesinger et al., 1996) or under selection pressure for neutralization-resistance (Beasley and Aaskov, 2001; Cecilia and Gould, 1991; McMinn et al., 1995a; Morita et al., 2001). Viruses with mutations at or near the hinge region frequently exhibit altered cultured cell infectivity or mouse virulence compared to their parental viruses; however, some of the previously studied mutant viruses contained additional mutations in other regions of the E protein, which made it difficult to fully elucidate the effect of the hinge mutations (Bray et al., 1998; Chambers and Nickells, 2001; Duarte dos Santos et al., 2000; Hasegawa et al., 1992; Lee et al., 1997; Ni et al., 2000). Only a few hinge mutations in JEV, DENV3, or MVEV have been demonstrated to individually affect virus phenotypes

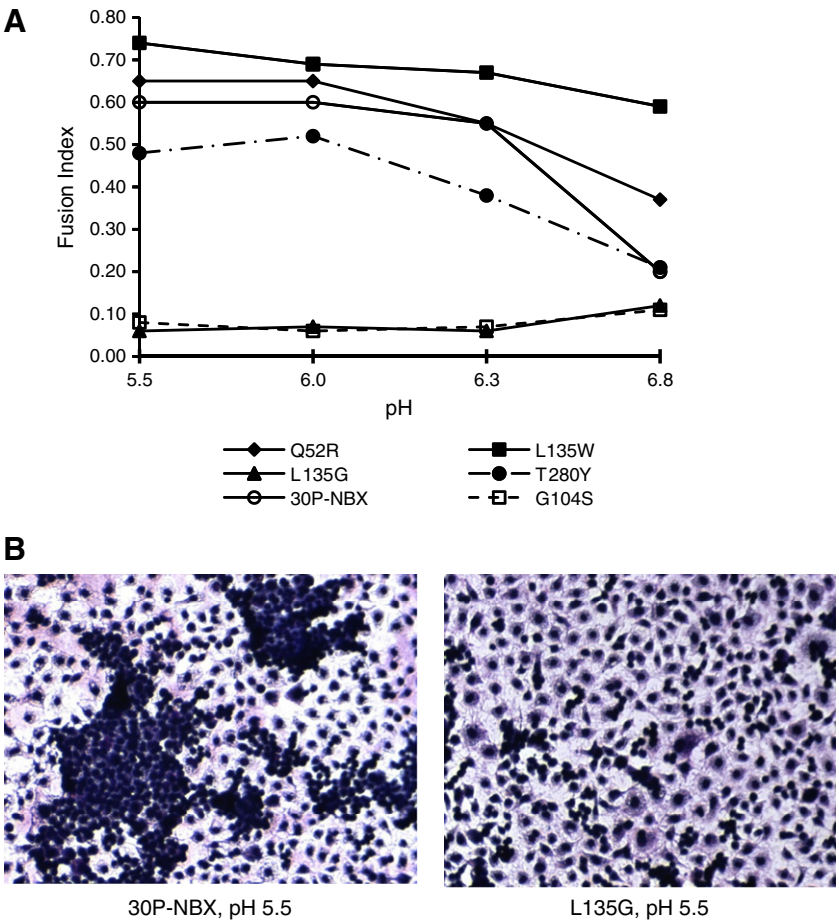

Fig. 4. FFWI assays in C6/36 cells. (A) Fusion curves showing 5 representative patterns. 1. 30P-NBX wt virus: fusion threshold pH 6.3–6.5; 2. Q52R: fusion threshold between pH6.3 and 6.5; 3. L135W: fusion pH threshold ≥6.8; 4. T280: fusion threshold between 6.0 and 6.3; 5. G104 and L135G: fusion negative. (B) Fusion photomicrographs of 30P-NBX and L135G at pH 5.5 stained with Hema-3 quick stain.

(Cecilia and Gould, 1991; Hurrelbrink and McMinn, 2001; Lee et al., 1997; Monath et al., 2002). In this study, using well defined mutant viruses derived from an infectious cDNA clone, we were able to identify nine new molecular determinants within the hinge region that can individually affect DENV2 infection in mammalian and mosquito cell cultures and in *Aedes aegypti* mosquitoes.

A Q52R mutation of JEV, combined with additional E protein mutations, was found to alter the structure of a neutralizing antibody epitope (Morita et al., 2001), early virus–cell interactions, and mouse virulence (Hasegawa et al., 1992). Interestingly, a G52R substitution is one of the mutations in the YFV 17D vaccine, and its neuroadapted variants with increased mouse virulence had multiple wt YFV reversions that included G52 (Chambers and Nickells, 2001). However, study of an intertypic recombinant virus showed that multiple reversions in E (including G52) and NS1 could not reconstitute the neurovirulence of the parental virus (Schlesinger et al., 1996). Our DENV2 Q52R mutation caused a shift of the fusion pH threshold to slightly higher than wt, and increased Vero cell-adaptation pressure that resulted in possible compensatory mutations at I277 (on H-4) and K122 (DII). The Q52 and I227 residues are very close to each other in the E protein pre-fusion dimer structure (Fig. 1C), and their side chains almost face each other in the monomers of the post-fusion trimer structure (data not shown). However, the mutation has no significant effect in infectivity for C6/36 cells or epitope structures recognized by multiple MAbs. Q52 may not be a major molecular determinant in the hinge region for DENV2 infection, but mutation at this locus could decrease the stability of the hinge structure and cause a lower energy requirement (higher pH) for membrane fusion. Substitution of A54, conserved among all flaviviruses, to a large acidic AA (E) shifted the fusion threshold to a higher pH and caused slightly delayed replication in Vero cells, suggesting A54 may also be important for stabilization of the functional hinge structure. Interestingly, in contrast to our observation, a DENV3 A54E mutant was previously shown to shift the fusion threshold to a slightly lower pH (decrease of 0.2 unit) (Lee et al., 1997). The difference in results may be due to the significant difference of the fusion pH threshold of parental virus between the two studies. The parental DENV3 used in the study of

Table 4
Monoclonal antibody reactivity of mutant L135G-infected Vero cells grown at 37 or 28 °C.

Antibody reactivity (Ab dilution fold at endpoint)*									
MAb Epitope	D2-NGC poly	1B4C-2 C1	4G2 A1	6B6C-1 A1	2H3 A4	1B7-5 A5	3H5 B1	9A3D-8 B2	1A1D-2 B4
37 °C	5120	**10**	**20**	<**10**	**40**	**20**	1280	**40**	640
28 °C	10240	40	2560	640	640	1280	2560	640	1280

* Antibody reactivity measured by IFA. Bold figures indicate greater than 4-fold difference from 28 °C cultures. There is no difference in the MAb reactivity with wt virus-infected cells grown at 37 or 28 °C.

Lee et al. had a neutral pH fusion threshold (pH 7.4–7.6), which is much higher than the fusion pH threshold of our wt DENV2 30P-NBX (pH 6.3–6.5). Mutation of A54V combined with other mutations in the YFV vaccine strain FNV, may also be responsible for the diminishing of its wt viscerotropic phenotype (Ni et al., 2000).

Mutations targeting the H-2 strand mosquito-borne flavivirus-conserved E133 and flavivirus-conserved L135 caused detrimental effects in virus infection of Vero cells. Mutation E133K was lethal in Vero cells and reverted to wt, and the C6/36 cell-derived E133K had a fusion pH threshold close to neutral pH. It is not surprising that substitution of conserved E133 (E side chain, pKa = 4.25) with an oppositely charged residue (K, pKa = 10.79) would significantly alter the fusion pH threshold. Unlike the results seen in Vero cells, the drastic change of the mosquito-borne flavivirus-conserved E133 to K did not affect its viability and replication efficiency in C6/36 cells, suggesting that the intracellular environment of Vero cells required a different mechanism for virus-mediated endosomal membrane fusion and/or viral maturation than the C6/36 cells. Such difference could explain why C6/36 cells were more susceptible than Vero cells to infection by most of our engineered DENV2 H mutants. This observation is consistent with our previous reports of other DENV2 mutants (Erb et al., 2010; Huang et al., 2010) and the general observation that wt DENVs usually replicate to much higher titers in C6/36 cells than in Vero or other mammalian cells.

The three L135 mutants had various phenotypic characteristics, and were quite different from the wt virus. The L135W virus could not replicate well in Vero cells until it reverted to wt or acquired compensatory mutations at other nearby hinge region residues. The large side chain of tryptophan likely decreased the stability of the hinge structure and resulted in a fusion pH threshold shift to more neutral pH. Although the mutant replicated well in C6/36 cells, it had a very low mosquito infection rate compared to wt virus. This supports our previous observations that infectivity of DENV for C6/36 mosquito cell cultures may not be an accurate model for predicting viral infectivity in whole mosquitoes (Erb et al., 2010; Huang et al., 2010). Changing L135 to K had no significant effect on fusion pH threshold; however, the virus replicated less efficiently in C6/36 cells than wt virus and evolved to 135M or acquired compensatory mutations in mammalian cells. Although L135K had a higher mosquito infection rate than mutant L135W, the infection rate was significantly lower than wt virus. Its evolution to 135M during passage of L135K in Vero cells (designated mutant L135M in Table 3) actually reconstituted the mosquito infectivity to that of wt virus. L135G was the most detrimental mutation tested among all the hinge mutations. The dramatic decrease in size of the AA side chain may have distressed the hydrophobic pocket structure lined by multiple hinge residues (Modis et al., 2003), and resulted in interrupting hinge functions for virus fusion and/or maturation. Indeed, the mutant failed to mediate membrane fusion over the entire pH range we tested in the FFWI assay. Our temperature shift assays and epitope mapping at 28 and 37 °C further support the notion that the 135G mutation altered the thermal stability of the E protein structures significantly at 37 °C. Interestingly, while exhibiting the most defective infectivity and fusion capacity in vitro, mutant L135G was able to infect *Ae. aegypti* by IT inoculation at a rate only slightly less than wt virus. This was not totally unexpected, considering that mosquitoes are incubated at 28 °C, where mutant L135G was more likely to maintain E protein structures required for productive mosquito tissue infection. The highly conserved L (or I) at position135 of all flaviviruses is likely an evolutionary result of their adaptation to both vertebrate hosts and arthropod vectors. In addition to determining that L135 is an important molecular determinant for DENV2 E protein hinge function and virus infectivity, we also identified possible interactions between hinge residues during the E protein conformational change and rearrangement by mapping the compensatory mutations that evolved during growth of mutants L135W and L135K in Vero and K562 cells (Fig. 1C). The possible interactions include AA residues 135 with 53 and/or 170, 135 with 186 and/or 276, and 135 with 265 (Fig. 1D). The interactions are likely physical, such as side-chain fit in the protein folding process, but there could also be chemical interactions, such as establishing H-bonds during refolding. Due to limited amounts of growth curve samples, we were not able to further characterize to what extent those compensatory mutations can restore the virus to wt phenotype. Future studies using genetically engineered mutants encoding these compensatory mutations will be necessary to fully elucidate the interactions of theses residues.

Although highly conserved among flaviviruses, H-3 G190 substitution with F or W did not affect mutant virus replication in mammalian or mosquito cell cultures. Mutant G190F maintained a similar fusion pH threshold, but the threshold for G190W shifted to a higher pH, suggesting that the bulkier W may reduce the stability of the hinge structure, resulting in requirement of less energy to initiate fusion. However, this position, residing close to the viral membrane at the pre-fusion stage (Fig. 1B), appears to be highly tolerant to substitutions of much larger residues. Switching large hydrophobic side chain F193 to a smaller A also did not significantly alter mutant replication in various cells. However, change of F193 to hydrophilic R significantly delayed virus replication in Vero cells until the engineered 193R population was partially replaced by 193L. A previous study of DENV3 discovered that mutation of F191 (DENV3 191 aligns with DENV2 193) to V or L occurs after multiple passages in Vero cells (Lee et al., 1997). It appears that a hydrophobic residue is required for residue 193, which lines the hydrophobic pocket (Modis et al., 2003).

Within the H-4 strand, we identified G266, I270, and G281as important molecular determinants for DENV2 replication in both mammalian and C6/36 cells. Although they are all fusion competent and only I270W showed a slight shift of the fusion pH threshold, these mutants did not replicate efficiently unless reversions or extra mutations were evolved in Vero cells. They also replicated to lower titers than wt virus in C6/36 cells. A somewhat different mutation, I270S, in a MAb neutralization-resistant JEV has been demonstrated to be a mouse attenuation determinant (Cecilia and Gould, 1991). Substitution of T280Y shifted the fusion threshold to a slightly lower pH and the mutant showed significantly lower fusion capacity than wt virus over the entire pH range. Unlike most other mutants in this study, mutant T280Y replicated less efficiently than wt virus in C6/36 cells, whereas it replicated similarly to wt virus in Vero cells. F279 is conserved among all DENVs, and a DENV3 F277S mutation (DENV3 AA277 aligns with DENV2 AA279) has been shown to significantly shift the fusion pH threshold in a FFWI assay (Lee et al., 1997). However, our DENV2 F279A mutation had no significant effect on the fusion pH threshold or virus infection in any of the cells we tested. Since F279 also participates in the hinge hydrophobic pocket structure, the residue likely requires a hydrophobic side chain such as F and A. Therefore, it is not surprising that mutation to hydrophilic S could alter the virus characteristics.

Epitope mapping of cells infected with these mutants identified mutations that altered MAb reactivity with all three E protein domains. The observation that changes at AA 135 altered MAb 1B4C-2 reactivity is the first direct evidence the C1 epitope resides in DI. It is interesting, but not surprising, that H-4 mutations altered the reactivity of MAb 2H3, which defines the A4 epitope on DII. It has been shown fairly conclusively that the DII epitope A1 is located in the fusion peptide, AA 98–110 (Crill and Chang, 2004; Huang et al., 2010). Competitive binding assays have shown that the A1 and A4 epitopes are not spatially related (Roehrig et al., 1998). Taken together, these data suggest that the A1 and A4 epitopes are likely located on the opposite ends of DII, placing A4 nearer DI and the H region. It should be noted, however, that the mutations in the H region likely could affect the conformation of the E protein and result in change of the reactivity to certain MAbs that bind at a distal site from the H region of the E protein homodimer. Therefore, we cannot conclude that any of

the H mutations are actually involved in the binding sites for those affected MAbs.

In summary, we analyzed 11 residues within the hinge region of DENV2, and identified nine of them (Q52, A54, E133, L135, F193, G266, I270, T280, and G281) as important molecular determinants in virus infection. None of these determinants has been examined in DENV2, and four of them (E133, L135, G266, and G281) have never been studied in any flavivirus. In addition, our results also provide the first evidence that mutation at L135 can profoundly decrease virus infection in whole mosquitoes. Although the region is highly susceptible to mutations and some residues seem to be tolerant to various substitutions, we have demonstrated particular properties of the determinants and possible residue contacts or interactions that are required to maintain the structure of the hinge for efficient virus infection. It has been proposed that the pocket structure of the flavivirus E protein hinge region would be an ideal target for development of anti-viral therapeutic molecules to block the hinge functions required for virus infection (Modis et al., 2003). Since the region is highly susceptible to mutation, our study provides more fundamental knowledge for evaluation of potential requirements for successful anti-viral molecule design.

Materials and methods

Cell culture

Vero, HepG2, and K526 cells were cultured at 37 °C, and C6/36 cells were cultured at 28 °C. Dulbecco's modified Eagle's medium (DMEM) was used for Vero and C6/36 cells, Eagle's minimum essential medium (EMEM) was used for culturing HepG2 cells (ATCC # HB-8065), and RPMI-1640 medium was used for K562 cells (ATCC # CCL-243). All growth media were supplemented with 10% fetal calf serum (FBS) for cell growth, and with 5% FBS for virus-infected cultures. Medium YE-LAH (0.165% lactalbumin hydrolysate, 0.033% yeast extract, Earl's balanced salt solution, 25 mg of gentamycin sulfate, and 1 mg of amphotericin B) with 5%FBS was used for virus propagation and growth studies in C6/36 cells.

Mutagenesis and recovery of mutant viruses

A DENV2 strain 16681 infectious cDNA plasmid, pD2/IC-30P-NBX, derived from pD2/IC-30P-A (Kinney et al., 1997), was used to construct all mutant clones as described previously (Huang et al., 2010). To derive viruses from infectious clones, in vitro transcribed full-length RNAs were transfected into Vero or C6/36 cells by electroporation as previously described (Huang et al., 2010). Following 10–12 days (Vero cells) or 14 days (C6/36 cells) of incubation, medium was harvested, clarified by centrifugation, adjusted to final 20% FBS, and stored at −70 °C for further studies. An aliquot was used to infect naïve cells and incubated for another 12–14 days to make working virus stock. Viability of the mutant virus was determined by indirect immunofluorescence assays (IFA) of viral antigens in infected cells and RT-PCR amplification of viral genome in cell cultures. Full-length genomes of the working seed viruses were sequenced to confirm their genetic stability. Viral RNA was extracted from seeds using QIAamp Viral RNA Kit (Qiagen), and amplified using Titan One Tube RT-PCR Systems Kit (Roche Applied Science, IN). The RT-PCR amplified fragments were purified before sequencing.

Growth kinetics and temperature sensitivity of mutant viruses in cell cultures

Twelve day growth curves were performed in Vero, HepG2, K562, and C6/36 cells. Temperature sensitivity tests were performed in Vero cell cultures at 28 or 37 °C for 12 days. Structural genes from day 12 samples of Vero and K562 growth curves as well as the Vero temperature sensitive experiment were sequenced to identify possible compensatory and/or cell-adaptive mutations evolved during the experiment. Cell cultures for growth kinetics and temperature sensitivity determinations were infected in duplicate at a multiplicity of infection (MOI) of 0.001 $TCID_{50}$, and viral genomic equivalents were measured by qRT-PCR (Butrapet et al., 2006). Samples with peak genomic equivalent titers were measured for infectious virus by $TCID_{50}$ in C6/36 cells (Huang et al., 2010).

Temperature shift assays

Four sets of freshly confluent Vero cells in 12-well tissue culture plates were infected with 0.5 ml of D2IC-30P-NBX or L135G virus at a MOI of 0.5. Two sets of plates were incubated at 28 °C and the other was kept at 37 °C for virus adsorption. After 2 h of virus absorption, cells were washed 3 times with PBS, and incubated with 2 ml fresh Iscove's DMEM medium. One set of the plates infected at 28 °C was maintained at 28 °C, while the other set was moved to 37 °C. Similarly, one set of plates infected at 37 °C was kept at 37 °C, but the other set was shifted to 28 °C for incubation. At selected time points (2, 24, 48, 72, 120 and 168 h) post-infection, 300 µl of culture medium were collected, and total intracellular RNA was extracted with Trizol reagent (Invitrogen) after the cells were washed twice with PBS. Triplicate samples were conducted for each time point. Quantities of viral genome in the collected culture medium were analyzed by qRT-PCR (Butrapet et al., 2006), and the intracellular negative-sense viral RNA was measured by a 2-step RT-qPCR using designed tagged primers to avoid false priming of positive-sense RNA as described previously (Huang et al., 2010).

Aedes aegypti mosquito infection by intrathoracic inoculation

Ae. aegypti RexD strain laboratory mosquitoes originating from Rexville, Puerto Rico, were reared from eggs and maintained as adults at 28 °C, 80% relative humidity with a photocycle of 12 h light:12 h dark. Intrathoracic (IT) inoculations were performed as described previously (Huang et al., 2010). Working virus seeds were diluted to 1×10^5 $TCID_{50}$/ml and adult female mosquitoes were IT inoculated with 0.3–0.5 µl of diluted virus. Injected mosquitoes were maintained for 7 days until head squashes were performed. Virus antigen was detected in head tissues by IFA to determine infection rates. Head squash IFAs were performed using flavivirus E protein DII group-reactive mouse MAb 4G2 as described previously (Brackney et al., 2008). Each IT injection experiment was repeated three times for a total of 81–143 mosquitoes for each virus. Head infectivity rates were determined by dividing the number of virus antigen-positive head squashes by the total number analyzed. To verify that no compensatory mutations developed in L135G infected mosquitoes, viral RNA was extracted from the saved body of a mosquito that was positive for virus antigen via head squash IFA, and the entire E gene was sequenced.

Antigenic characterization of mutant E proteins

E protein reactivity of a panel of DENV and flavivirus MAbs (Roehrig et al., 1998), including 1B4C-2 (C1 epitope, in E protein DI), 4G2 and 6B6C-1(A1 epitope, DII), 2H3 (A4 epitope, DII), 1B7-5 (A5 epitope, DII), 3H5 (B1 epitope, DIII), 9A3D-8 (B2 epitope, DIII), and 1A1D-2 (B4 epitope, DIII), was compared to reactivity with wt D2IC-30P-NBX by IFA with acetone-fixed virus-infected C6/36 cells (Huang et al., 2010). In addition, epitope expression of mutant L135G E protein at 28 and 37 °C was compared in Vero cells. For this analysis, duplicate Vero cell cultures were infected with mutant L135G at 28 °C for 2 h. After washing the cells 3 times with PBS, fresh medium was added, and one flask of infected cells was incubated at 28 °C and the other at 37 °C. Cells in the 37 °C flask were harvested after 24 h of infection, and the cells kept at 28 °C were harvested 4 days later. Infected cells were gently scraped off after PBS

wash, dropped on poly-L-lysine coated slides, air dried, and fixed in cold acetone. IFA with D2-NGC polyclonal antibody (mouse hyperimmune ascitic fluid) was included as a control to normalize different activities (within 2-fold) due to different amounts of intracellular E proteins expressed at the two temperatures (Table 4). Results were averages of the end point dilution of MAbs from 2 separate experiments.

Fusion from within (FFWI) assay

Fusion activity was measured by quantitating cell–cell fusion of virus-infected C6/36 cells as previously described (Guirakhoo et al., 1993; Huang et al., 2010). Briefly, C6/36 cells in 24-well plates were infected at MOI of 0.1 and maintained in pH 7.7 medium at 28 °C. At day 7 post-infection when almost all cells would be infected, cell medium was replaced by fusion medium buffered between pH 5.5 and 6.8, and incubated for 2 h at 28 °C. Cells were returned to pH 7.7 medium for additional 24 h incubation and stained with Hema-3 quick stain (Fig. 4B). Numbers of cells and nuclei were counted and fusion index (FI) was calculated as previously reported (Huang et al., 2010). Fusion curves were plotted as mean FI from at least 2 experiments for each pH (Fig. 4A), and fusion pH threshold range was shown as FI ≥ 0.5 (Table 1). Fusion activity at pH5.5 was calculated to determine overall fusion capacity of each mutant (Table 1). Triplicate mock-infected cell controls and wt 30P-NBX controls were included in each experimental plate for calibration of the fusion activity at pH 5.5. Fusion activity at pH 5.5 = (mutant FI – mock cell FI) / (30P-NBX FI – mock cell FI). The standard deviation was calculated from triplicate samples of each virus.

Acknowledgments

We thank Mr. Rich Tsuchiya and Shawn Silengo for assistance in viral genome sequencing. We also thank Frank Cooney for his assistance in E epitope mapping. This study was supported by Centers for Disease Control and Prevention and grants from Pediatric Dengue Vaccine Initiative (PDVI TR-159A) and the CSU College of Veterinary Medicine and Biomedical Sciences Research Council.

References

Beasley, D.W., Aaskov, J.G., 2001. Epitopes on the dengue 1 virus envelope protein recognized by neutralizing IgM monoclonal antibodies. Virology 279 (2), 447–458.
Brackney, D.E., Foy, B.D., Olson, K.E., 2008. The effects of midgut serine proteases on dengue virus type 2 infectivity of Aedes aegypti. Am. J. Trop. Med. Hyg. 79 (2), 267–274.
Bray, M., Men, R., Tokimatsu, I., Lai, C.J., 1998. Genetic determinants responsible for acquisition of dengue type 2 virus mouse neurovirulence. J. Virol. 72 (2), 1647–1651.
Bressanelli, S., Stiasny, K., Allison, S.L., Stura, E.A., Duquerroy, S., Lescar, J., Heinz, F.X., Rey, F.A., 2004. Structure of a flavivirus envelope glycoprotein in its low-pH-induced membrane fusion conformation. EMBO J. 23 (4), 728–738.
Butrapet, S., Kinney, R.M., Huang, C.Y., 2006. Determining genetic stabilities of chimeric dengue vaccine candidates based on dengue 2 PDK-53 virus by sequencing and quantitative TaqMAMA. J. Virol. Meth. 131 (1), 1–9.
Cecilia, D., Gould, E.A., 1991. Nucleotide changes responsible for loss of neuroinvasiveness in Japanese encephalitis-virus neutralization-resistant mutants. Virology 181 (1), 70–77.
Chambers, T.J., Nickells, M., 2001. Neuroadapted yellow fever virus 17D: genetic and biological characterization of a highly mouse-neurovirulent virus and its infectious molecular clone. J. Virol. 75 (22), 10912–10922.
Chu, J.J., Ng, M.L., 2004. Infectious entry of West Nile virus occurs through a clathrin-mediated endocytic pathway. J. Virol. 78 (19), 10543–10555.
Crill, W.D., Chang, G.J., 2004. Localization and characterization of flavivirus envelope glycoprotein cross-reactive epitopes. J. Virol. 78, 13975–13986.
Duarte dos Santos, C.N., Frenkiel, M.P., Courageot, M.P., Rocha, C.F., Vazeille-Falcoz, M.C., Wien, M.W., Rey, F.A., Deubel, V., Despres, P., 2000. Determinants in the envelope E protein and viral RNA helicase NS3 that influence the induction of apoptosis in response to infection with dengue type 1 virus. Virology 274 (2), 292–308.
Erb, S.M., Butrapet, S., Moss, K.J., Luy, B.E., Childers, T., Calvert, A.E., Silengo, S.J., Roehrig, J.T., Huang, C.Y.-H., Blair, C.D., 2010. Domain-III FG loop of the dengue virus type 2 envelope protein is important for infection of mammalian cells and Aedes aegypti mosquitoes. Virology.
Gollins, S.W., Porterfield, J.S., 1985. Flavivirus infection enhancement in macrophages: an electron microscopic study of viral cellular entry. J. Gen. Virol. 66 (Pt 9), 1969–1982.
Guirakhoo, F., Hunt, A.R., Lewis, J.G., Roehrig, J.T., 1993. Selection and partial characterization of dengue 2 virus mutants that induce fusion at elevated pH. Virology 194 (1), 219–223.
Hasegawa, H., Yoshida, M., Shiosaka, T., Fujita, S., Kobayashi, Y., 1992. Mutations in the envelope protein of Japanese encephalitis virus affect entry into cultured cells and virulence in mice. Virology 191 (1), 158–165.
Heinz, F.X., 1986. Epitope mapping of flavivirus glycoproteins. Adv. Virus Res. 31, 103–168.
Huang, C.Y., Butrapet, S., Moss, K.J., Childers, T., Erb, S.M., Calvert, A.E., Silengo, S.J., Kinney, R.M., Blair, C.D., Roehrig, J.T., 2010. The dengue virus type 2 envelope protein fusion peptide is essential for membrane fusion. Virology 396 (2), 305–315.
Hurrelbrink, R.J., McMinn, P.C., 2001. Attenuation of Murray Valley encephalitis virus by site-directed mutagenesis of the hinge and putative receptor-binding regions of the envelope protein. J. Virol. 75 (16), 7692–7702.
Kinney, R.M., Butrapet, S., Chang, G.J., Tsuchiya, K.R., Roehrig, J.T., Bhamarapravati, N., Gubler, D.J., 1997. Construction of infectious cDNA clones for dengue 2 virus: strain 16681 and its attenuated vaccine derivative, strain PDK-53. Virology 230, 300–308.
Kuhn, R.J., Zhang, W., Rossmann, M.G., Pletnev, S.V., Corver, J., Lenches, E., Jones, C.T., Mukhopadhyay, S., Chipman, P.R., Strauss, E.G., Baker, T.S., Strauss, J.H., 2002. Structure of dengue virus: implications for flavivirus organization, maturation, and fusion. Cell 108, 717–725.
Lee, E., Weir, R.C., Dalgarno, L., 1997. Changes in the dengue virus major envelope protein on passaging and their localization on the three-dimensional structure of the protein. Virology 232 (2), 281–290.
Mandl, C.W., Guirakhoo, F., Holzmann, H., Heinz, F.X., Kunz, C., 1989. Antigenic structure of the flavivirus envelope protein E at the molecular level, using tick-borne encephalitis virus as a model. J. Virol. 63 (2), 564–571.
McMinn, P.C., Lee, E., Hartley, S., Roehrig, J.T., Dalgarno, L., Weir, R.C., 1995a. Murray valley encephalitis virus envelope protein antigenic variants with altered hemagglutination properties and reduced neuroinvasiveness in mice. Virology 211 (1), 10–20.
McMinn, P.C., Marshall, I.D., Dalgarno, L., 1995b. Neurovirulence and neuroinvasiveness of Murray Valley encephalitis virus mutants selected by passage in a monkey kidney cell line. J. Gen. Virol. 76 (Pt 4), 865–872.
Modis, Y., Ogata, S., Clements, D., Harrison, S.C., 2003. A ligand-binding pocket in the dengue virus envelope glycoprotein. Proc. Natl Acad. Sci. USA 100 (12), 6986–6991.
Modis, Y., Ogata, S., Clements, D., Harrison, S.C., 2004. Structure of the dengue virus envelope protein after membrane fusion. Nature 427 (6972), 313–319.
Modis, Y., Ogata, S., Clements, D., Harrison, S.C., 2005. Variable surface epitopes in the crystal structure of dengue virus type 3 envelope glycoprotein. J. Virol. 79 (2), 1223–1231.
Monath, T.P., Arroyo, J., Levenbook, I., Zhang, Z.X., Catalan, J., Draper, K., Guirakhoo, F., 2002. Single mutation in the flavivirus envelope protein hinge region increases neurovirulence for mice and monkeys but decreases viscerotropism for monkeys: relevance to development and safety testing of live, attenuated vaccines. J. Virol. 76 (4), 1932–1943.
Morita, K., Tadano, M., Nakaji, S., Kosai, K., Mathenge, E.G., Pandey, B.D., Hasebe, F., Inoue, S., Igarashi, A., 2001. Locus of a virus neutralization epitope on the Japanese encephalitis virus envelope protein determined by use of long PCR-based region-specific random mutagenesis. Virology 287 (2), 417–426.
Mosso, C., Galvan-Mendoza, I.J., Ludert, J.E., del Angel, R.M., 2008. Endocytic pathway followed by dengue virus to infect the mosquito cell line C6/36 HT. Virology 378 (1), 193–199.
Ni, H., Ryman, K.D., Wang, H., Saeed, M.F., Hull, R., Wood, D., Minor, P.D., Watowich, S.J., Barrett, A.D.T., 2000. Interaction of yellow fever virus French neurotropic vaccine strain with monkey brain: characterization of monkey brain membrane receptor escape variants. J. Virol. 74 (6), 2903–2906.
Rey, F.A., Heinz, F.X., Mandl, C., Kunz, C., Harrison, S.C., 1995. The envelope glycoprotein from tick-borne encephalitis virus at 2 A resolution. Nature 375 (6529), 291–298.
Roehrig, J.T., Bolin, R.A., Kelly, R.G., 1998. Monoclonal antibody mapping of the envelope glycoprotein of the dengue 2 virus, Jamaica. Virology 246 (2), 317–328.
Roehrig, J.T., Johnson, A.J., Hunt, A.R., Bolin, R.A., Chu, M.C., 1990. Antibodies to dengue 2 virus E-glycoprotein synthetic peptides identify antigenic conformation. Virology 177 (2), 668–675.
Schlesinger, J.J., Chapman, S., Nestorowicz, A., Rice, C.M., Ginocchio, T.E., Chambers, T.J., 1996. Replication of yellow fever virus in the mouse central nervous system: comparison of neuroadapted and non-neuroadapted virus and partial sequence analysis of the neuroadapted strain. J. Gen. Virol. 77 (Pt 6), 1277–1285.
Stiasny, K., Bressanelli, S., Lepault, J., Rey, F.A., Heinz, F.X., 2004. Characterization of a membrane-associated trimeric low-pH-induced Form of the class II viral fusion protein E from tick-borne encephalitis virus and its crystallization. J. Virol. 78 (6), 3178–3183.
Stiasny, K., Kossl, C., Lepault, J., Rey, F.A., Heinz, F.X., 2007. Characterization of a structural intermediate of flavivirus membrane fusion. PLoS Pathog. 3 (2), e20.
van der Schaar, H.M., Rust, M.J., Chen, C., van der Ende-Metselaar, H., Wilschut, J., Zhuang, X., Smit, J.M., 2008. Dissecting the cell entry pathway of dengue virus by single-particle tracking in living cells. PLoS Pathog. 4 (12), e1000244.
Wang, E., Ryman, K.D., Jennings, A.D., Wood, D.J., Taffs, F., Minor, P.D., Sanders, P.G., Barrett, A.D.T., 1995. Comparison of genomes of the wild-type French viscerotropic strain of yellow fever virus with its vaccine derivative French neurotropic vaccine. J. Gen. Virol. 76, 2749–2755.
Zhang, W., Chipman, P.R., Corver, J., Johnson, P.R., Zhang, Y., Mukhopadhyay, S., Baker, T.S., Strauss, J.H., Rossmann, M.G., Kuhn, R.J., 2003. Visualization of membrane protein domains by cryo-electron microscopy of dengue virus. Nat. Struct. Biol. 10 (11), 907–912.
Zhang, Y., Zhang, W., Ogata, S., Clements, D., Strauss, J.H., Baker, T.S., Kuhn, R.J., Rossmann, M.G., 2004. Conformational changes of the flavivirus E glycoprotein. Structure 12 (9), 1607–1618.